MAX 4^U, AN UPGRADE OF THE MAX IV 3 GeV RING*

E. Al-Dmour†, M. B. Alves, Å. Andersson, M. Apollonio, J. Bengtsson, F. Cullinan, H. O. C. Duarte, M. Grabski, O. Karis, R. Lindvall, E. Mansten, S. Molloy, A. Robert, J. Schnadt, A. Sharma, M. Sjöström, H. Tarawneh, P. Tavares, S. Thorin, K. Åhnberg
MAX IV Laboratory, Lund, Sweden

Abstract

The MAX IV 3 GeV storage ring in Lund, Sweden, was the first implementation of a multibend achromat (MBA) lattice fourth-generation light source. Since it started delivery of light in 2016, several succeeding MBA-based rings and variants have come on-line and many others are being planned, designed, built or commissioned. All of these capitalise on the MBA concept and expand it to push the brightness and coherence performance even further. In order to continue to offer competitive tools to the Swedish and international scientific communities beyond the end of this decade, MAX IV Laboratory launched in 2024 the conceptual design work of MAX 4^U, an upgrade of its 3 GeV storage ring with the goal of an emittance below 100 pm rad. This performance boost is to be achieved through a minimum-interference upgrade in which localised interventions in selected subsystems and components are carefully chosen to provide the maximum performance increase with minimum cost and, equally important, minimum dark time for the MAX IV user community. In 2025, the conceptual design report (CDR) was completed, and the focus in 2026 is to elaborate on the solutions identified for this upgrade through the Technical Design Report (TDR), to be completed by the end of 2028. This contribution describes the latest developments in accelerator physics and engineering aspects of the MAX 4^U design.

INTRODUCTION

MAX IV Laboratory is a Swedish national synchrotron laboratory located in Lund, Sweden. MAX IV Laboratory consists of a 3 GeV and a 1.5 GeV storage ring and a linear accelerator that serves as an injector to both rings as well as a driver for our Short Pulse Facility (SPF). The existing 3 GeV storage ring (R3), the first fourth-generation storage ring in the world, employs a multibend achromat (MBA) lattice enabling a bare lattice emittance of 328 pm rad [1]. Since the MAX IV inauguration in 2016, the storage ring landscape has changed, with several multibend-achromat facilities with reduced emittance now operating worldwide and more underway. Furthermore, the next phase of beamlines that are part of the MAX IV roadmap foresees up to five new beamlines, which are critically dependent on brightness and coherence, which in turn depend on reducing the electron beam emittance. To meet this challenge, MAX IV initiated the conceptual design studies for MAX 4^U in 2024, aiming to upgrade the 3 GeV ring by reducing its emittance to below 100 pm rad, while preserving the energy at 3 GeV, maintaining the source points, the shielding wall and the injector, all within strict cost and time constraints. In December 2025, the Conceptual Design Report (CDR) was completed [2–4]. The main conclusion was to bring the emittance target for the technical design phase for MAX 4^U from 100 pm rad down to 75 pm rad, with all other boundary conditions maintained. The following sections describe the present status of the project focusing on the lattice design that is the basis for the TDR work.

BEAM DYNAMICS

Lattice Design

As the TDR phase of MAX 4^U began at the start of 2026, the lattice design work narrowed to a single lattice candidate named TDR-1, which is an evolution of the CDR lattices. Consequently, as for the latter, the emittance decrease relative to R3 has been achieved primarily by the introduction of reverse bends as illustrated in Fig. 1. The overall structure

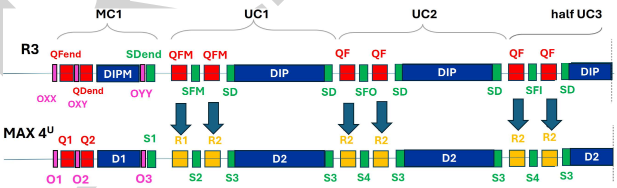

Figure 1: Layout of half an achromat for R3 and MAX 4^U. The different magnets are color-coded: quadrupoles (red), combined-function dipoles (blue), reverse bends (orange), sextupoles (green), and octupoles (magenta).

is retained in order to preserve beamline source points and reuse as much of the existing installation and equipment as possible. Thus, the TDR-1 lattice remains a 7-bend achromat lattice with a periodicity of 20.

That stated, designing an accelerator lattice is always an exercise in multi-objective optimisation. For the TDR-1, these objectives include the usual lattice performance parameters such as emittance, insertion device (ID) straight section beta functions, lifetime and injection efficiency. It should be noted that the intended use of an off-phase/on-axis injection method shifts the relative weights put on the dynamic aperture and the momentum and phase acceptance. The optimisation objectives also include certain engineering parameter thresholds beyond which cost and/or complexity for the upgrade is significantly affected. An example of

* We acknowledge funding from The Crafoord Foundation (Crafoordska stiftelsen) (Grant 20250007).
† eshraq.al-dmour@maxiv.lu.se

PREPRINT

this is the matching cell bend angle, which, if lower than 1.4°, will necessitate the replacement of additional vacuum chambers in that cell. It is important to note that the lattice design is proceeding in parallel with the engineering work, this results in a somewhat fluid process where optimisation objectives can and do change in relevance; the engineering and lattice work guide each other. The main tools used by the lattice design have been the Accelerator Toolbox [5], Tracy 3.5 [6], and Thor [7,8]; additional codes such as elegant [9] and OPA [10] have been used for cross-checks. The main parameters of the current TDR-1 lattice are presented in Table 1, while the machine functions can be seen in Fig. 2. The dynamic aperture and separatrix are found in Fig. 3 and Fig. 4, respectively. Finally, the effect of Intra-Beam Scattering (IBS) is shown in Fig. 5.

Table 1: Parameters for MAX 4$^{\mathrm{U}}$ TDR-1, Bare Lattice

Parameter	**MAX 4$^{\mathrm{U}}$**
Energy (GeV)	3.0
Circumference (m)	528.096
Achromat angle (deg.)	18
Tunes ν_x, ν_y	(58.32, 17.17)
Current (mA)	500
Average β_x, β_y (m)	(3.18, 6.13)
Average η_x (m)	0.0165
ξ_x, ξ_y	(2, 2)
Momentum comp. α_1, α_2 (10^{-4})	0.53, 3.6
Energy loss per turn (keV)	474.1
Nat. energy spread (%)	0.08
Nat. emittance (pm rad)	65.2

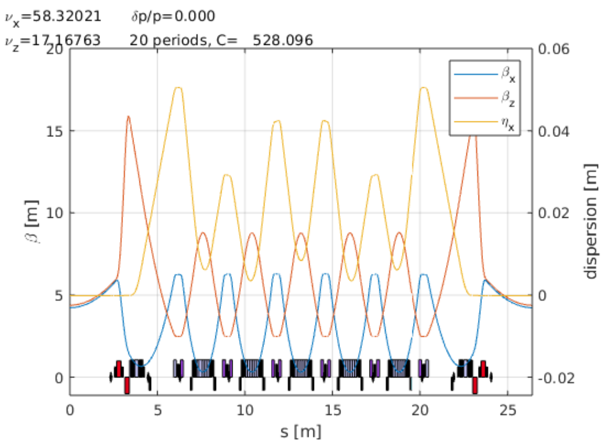

Figure 2: Linear optics functions for the MAX 4$^{\mathrm{U}}$ TDR-1 lattice.

Error Model and Simulated Commissioning

The achievable lattice performance greatly depends on the accuracy of girder and magnet manufacturing and alignment, as well as the available methods to compensate for the remaining errors. In order to include this aspect in the design process early on, error models were established based on experience from the production, installation and alignment

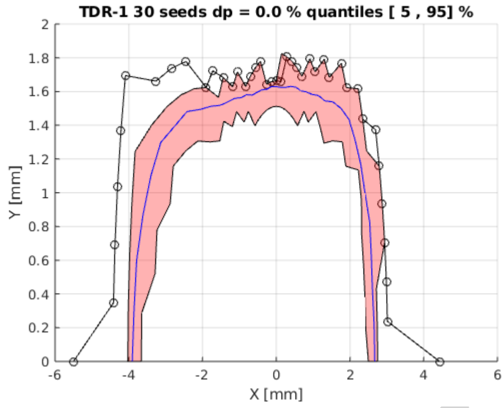

Figure 3: Dynamic aperture.

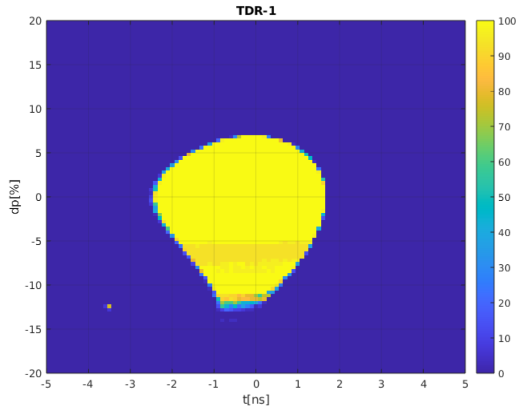

Figure 4: Longitudinal phase space acceptance. Yellow regions indicate initial conditions for which injected electrons (at close to zero transverse coordinates) are captured in the ring, whereas blue regions indicate initial conditions where electrons are lost. Calculations are done with 30 error seeds, and the colour code indicates the fraction (in %) of all seeds at which particles survive.

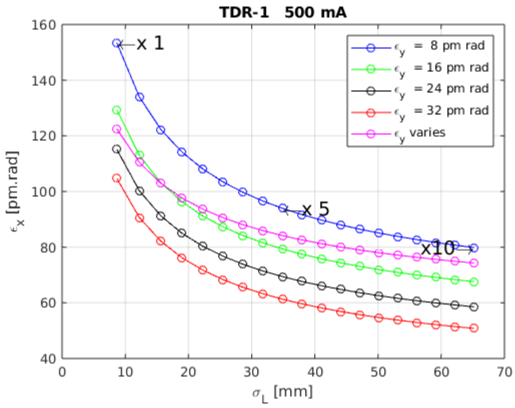

Figure 5: Intrabeam Scattering impact on the horizontal emittance under different scenarios for the vertical emittance, which may be set by fine-tuning of the transverse emittance coupling, and bunch length. In particular, the impact of the bunch stretching is indicated.

DRAFT

of the R3 magnets, as well as the accelerator operation since then [2]. As the full simulated commissioning toolbox was not available, an approximate model reflecting the achievable orbit and machine function errors after correction in R3 was also produced and has been used throughout the design phase. Work on the full simulated commissioning is ongoing; once it is ready the lattice design will change to utilising the full error model.

Collective Effects

The evaluation of collective effects for MAX 4^U combines an impedance model of R3 with beam-based measurements, motivated by the reuse of most vacuum chambers. Since the impedance model is known to underestimate measurements, experimental data are used to rescale the predictions. The analysis considers a target design current of 500 mA with a uniform fill pattern (corresponding to 2.84 mA per bunch for 176 bunches), focusing on single-bunch instabilities (Transverse Mode-Coupling Instability (TMCI) and microwave instability) as well as coupled-bunch instabilities driven by the fundamental modes of rf cavities. The reduced momentum compaction factor in the upgrade lattice systematically lowers instability thresholds compared to R3, making accurate scaling and mitigation strategies essential. For transverse stability, TMCI thresholds are derived by mapping R3 measurements to the upgrade lattice. At zero chromaticity, the thresholds are reduced due to the lower momentum compaction, but increase more rapidly with chromaticity, allowing recovery of operational margins. With IDs closed, the thresholds are reduced by approximately a factor of two, requiring chromaticities of about 0.7 to maintain sufficient stability margin, while the lattice design accommodates operation up to chromaticities of +2. Additional margin can be provided by transverse bunch-by-bunch feedback, if required. In the longitudinal plane, the broadband impedance leads to potential-well distortion and microwave instability. The predicted microwave instability threshold is about 1.6 mA without harmonic cavities, increasing only to 1.7 mA with ideal bunch lengthening in a double-rf system. At the design current, the TDR-1 lattice is therefore expected to operate above the microwave instability threshold, though with a limited energy spread increase of about 13 %. Studies on mitigation strategies to increase the threshold above the design bunch current are ongoing. Bunch lengthening using harmonic cavities is critical for reducing impedance-induced heating, mitigating emittance blow-up due to intrabeam scattering (see Fig. 5), enhancing Touschek lifetime, and improving stability against higher-order modes from the rf cavities. A double-rf system with passive 300 MHz or 500 MHz cavities is already in use in R3 today and a triple-rf system combining all these frequencies (100 (main rf frequency), 300, and 500 MHz) could in principle, provide significantly larger bunch lengthening. Stability analysis shows that the mode-1 coupled-bunch instability driven by the harmonic cavity impedance is the main limitation in all these variants: using two 300 MHz cavities would restrict the total current to below 250 mA, whereas a single cavity allows stable operation at 500 mA. Mode-0 (Robinson) instabilities are expected to be controlled with a dedicated mode-0 damper installed in the 100 MHz cavities, as existent in R3. For typical operating conditions (with 1.0–1.4 MV of main rf voltage, for different energy losses from IDs radiation), stable solutions with bunch lengthening factors of about 3–6 are obtained using a double-rf system, in good agreement between semi-analytical methods and macroparticle tracking [11]. Overall, the studies indicate that a stable operation at the design current is feasible provided the harmonic cavity impedance is minimised, rf parameters are optimised, and appropriate feedback systems are implemented.

MAGNET SYSTEM

The R3 magnet system consists of 20 multi-bend achromats, each containing seven cells [1]. Each cell is a precision-machined iron block designed to accommodate different types of magnet elements. The MAX 4^U magnet system is being designed based on the same modular concept as for R3. Compared with the standard MAX IV lattice, the TDR-1 lattice requires higher integrated strengths for most of the magnets. It also requires a new magnet family, the reverse bend magnet. The magnet aperture for MAX 4^U is 25 mm in diameter, the same as for R3, which allows retaining existing vacuum chambers. The electromagnetic design of Dipole D2, Reverse Bend R2, Quadrupoles Q1 and Q2, and Sextupoles S1, S2, S3, and S4 has been completed for the MAX 4^U TDR-1 lattice [12]. The octupole and corrector magnets can retain the R3 designs. The design of the remaining magnets is currently in progress, and the magnetic cross-talk simulations between neighbouring magnets within the cells are also being evaluated. A full-scale prototype of a Unit Cell is planned; the prototyping program will help assess manufacturing feasibility and validate improvements introduced in the unit cell iron block design based on lessons learned from the R3 magnet system. Extensive magnetic measurements will be carried out to validate the magnet designs and to develop measurement and assessment procedures for the new reverse bend magnets integrated within the unit cell. Crosstalk measurements with neighbouring magnets will also be performed to evaluate magnet behaviour under realistic operating conditions. In addition, a full-scale prototype dipole magnet based on permanent magnets is currently being manufactured [13].

INJECTION SYSTEM

The MAX IV injector is based on a full-energy linear accelerator (linac), consisting of 39 normal-conducting S-band 3 GHz linac sections together with 19 rf units, each comprising a 35 MW klystron and a solid-state modulator [14]. Currently, two storage-ring injection schemes are in operation, using either a thermionic rf gun or a photocathode gun. In the thermionic mode, a chopper system, in combination with an energy filter and stripline kickers, selects a train of bunches matched to the 100 MHz rf buckets of the storage ring [15]. Alternatively, a photocathode gun can be

PREPRINT

used to generate a single linac rf bucket electron bunch with around 200 pC charge. Since the 3 GHz linac frequency is not a multiple of the 100 MHz ring rf, a coincidence timing system is required. In this scheme, a coincidence detector triggers the linac when a ring bucket temporally overlaps with a potential photocathode laser pulse. Photo-cathode gun injection provides high precision by producing bunches with a time duration of a few picoseconds, low emittance, and low energy spread. At present, both schemes use a multipole injection kicker (MIK) [16] to place the injected beam onto the correct injection trajectory. The combination of large bunch spacing in the 100 MHz rf system, together with the photocathode gun precision and the full-energy linac, enables the implementation of off-phase, on-axis injection schemes [17, 18]. This improves top-up transparency, allows the use of IDs with small horizontal gaps, and enables accumulation in limited dynamic aperture lattices. Another option for injection would be with a MIK upgrade with a suitable transverse field profile to allow for transverse injection within the dynamic aperture of MAX 4^U lattice. The realisation of off-phase, on-axis injection requires fast stripline kickers driven by high-voltage pulsers to place the injected bunch on axis without disturbing the stored beam. For MAX 4^U, the fall time of the stripline kicker pulse needs to be below 2 ns while still reaching a peak voltage of at least 20 kV. This requires several short stripline modules to achieve the required kick.

RF SYSTEM

The 100 MHz rf system of R3 is described in [19]. Operating at a comparatively low frequency, a key advantage of the rf system in the context of MAX 4^U is that it provides a 10 ns spacing between consecutive bunches. For the purpose of estimating rf power needs, we assume that the energy loss per turn from 18 operational IDs will eventually reach 326 keV/turn, this added to the dipole and reverse bend losses (474 keV/turn) will give a maximum of 800 keV/turn. The new lattice, TDR-1, have a smaller momentum compaction, and thus will require lower rf fields, which also reduces the required rf power. We estimate more than 20 % lower rf power consumption for MAX 4^U compared to R3. Thus, there is a possibility to go from the original six cavity system to a five cavity system, which would allow for easy and fast backup solutions, in case of issues with either a cavity, a circulator or a transmitter. Table 2 summarises the design parameters for the rf systems for R3 and MAX 4^U TDR-1 lattice.

The rf momentum acceptance has larger and asymmetric values in view of allowing for off-phase injection and taking into account second-order momentum compaction. One should note that the optimum coupling is calculated with the Landau cavity powers in mind. The foreseen dual harmonic cavity system, will consist of what is described in Table 2, plus an additional actively driven harmonic cavity at 500 MHz. It is conveniently realised by being the well-established HOM-damped EU-cavity, being in operation at several facilities. With such a system, we expect a bunch lengthening factor between five and ten, when adjusting to, or nearby to, the super-flat condition [3].

Table 2: Design Parameters for the RF Systems in R3 and in MAX 4^U

Parameter	**R3**	**MAX 4^U**
Energy loss per turn (MeV)	1	0.8
Momentum Acceptance (%)	±4.5	(−14.7, 7.4)
Momentum Compaction (10^{-4})	3.06	0.53
Current (mA)	500	500
Total SR Power (kW)	500	400
Main rf System		
Total rf Voltage (MV)	1.8	1.4
Number of Cavities	6	5
Cavity Voltage (kV)	300	280
Cavity $R_{sh}(= V^2/P)$ (MΩ)	3.2	3.4
Total cavity losses (kW)	169	115
Optimum Coupling	4.05	4.70
Number of rf stations	6	5
Min. rf station power (kW) (with LC losses)	114	108
Landau Cavity System 300 MHz		
Total LC Voltage (kV)	487	371
Number of Cavities	3	1
LC $R_{sh}(= V^2/P)$ (MΩ)	5	5.34
Total LC losses (kW)	16	26

VACUUM SYSTEM

Due to the addition of reverse bends in TDR-1, the electron orbit has changed relative to R3. To accommodate this new orbit, changes to the vacuum chambers will be required in the matching cells (MC1, MC2) and short straight section (SS1) of each achromat. Following the work on the vacuum system reported in the CDR, and as the MC1 and MC2 bending angles exceed 1.4°, around 30 % of the vacuum chambers (lengthwise) in each arc will need to be replaced with new ones [20]. The design will follow a similar concept as R3 [21, 22]. The new chambers will be very similar to the R3 chambers; they will be made of copper, coated with non-evaporable getter (NEG), have circular cross-section and water cooling to dissipate the power from synchrotron radiation. The remaining 70 % of the arc vacuum chambers are to be reused, with their geometry adjusted (bent) to fit the new orbit. The vacuum system of the long straight sections for the IDs will remain intact. To install the new vacuum chambers and adapt the geometry of the existing ones, each arc will need to be vented and then baked, and NEG coating reactivated. Currently, the vacuum system installation procedure is being developed with the goal of shortening the needed time as much as possible to minimise the impact on the dark period. Therefore, the possibility of activating the NEG-coated vacuum chambers of a complete arc in-situ (with removed magnets), without venting the long

PREPRINT

PREPRINT

straight sections for the IDs, is studied. The procedure must take into account the following boundary conditions: (i) the vacuum chambers will expand during NEG activation at 180 °C, accordingly, the vacuum vessels and bellows should safely accommodate this; (ii) the old magnet blocks will be removed and new ones installed while the vacuum chambers remain in place; (iii) a portion of the vacuum chambers will be replaced with new ones, and several will be reused and their geometry mechanically adapted to the new orbit; and (iv) the beam position monitors (BPM) and vacuum vessel positions are defined by the magnet block positions.

Simulations and studies are done, with new equipment and tooling being developed to meet the challenges this procedure will impose.

MECHANICAL INTEGRATION

During the CDR work [2, 3, 23], a process was developed to enable a quick evaluation of vacuum chambers following a new beam path. At a conceptual level, the vacuum system components and the magnets for MAX 4^U remain the same as for R3. Studies have been carried out to verify the feasibility of many different lattice alternatives. The selection of a lattice (TDR-1) provides the stability to start working on a more detailed design of components. Vacuum chambers and magnets are being developed in parallel in a parametrised way with the lattice as a backbone, connecting the different components to the beam path and allowing for future changes of the beam path without redesign. Once the models are complete, a detailed interference check will be performed with 0.5 mm clearance between magnets and vacuum components and 3 mm between the magnet coils and vacuum components. A mock-up is being planned to test installation procedures, tooling and prototypes. Equipment for handling the installation of magnet blocks with the vacuum system in place and tools for in-situ bending of vacuum chambers are being developed.

INSERTION DEVICES

The performance of MAX 4^U IDs was evaluated at the CDR phase [2]. The analysis focuses on key metrics such as brilliance, coherence, flux, power density, and operational impact on beamlines. Importantly, existing and funded IDs can operate unchanged in MAX 4^U as beam energy, aperture, and K-values remain the same. A wide range of IDs is considered, including APPLE II, quasi-APPLE II, APPLE X, in-vacuum undulators (IVU), cryogenic permanent magnet undulators (CPMU), and wigglers. Performance estimates rely on measured magnetic fields and updated beam parameters. Figure 6 shows the impact of the reduction of the beam emittance on the horizontal coherent fraction based on 65.2 pm rad natural emittance with coupling of 14%. In the soft X-ray regime, APPLE II undulators (EPU) benefit significantly from improved horizontal coherence and brilliance, achieving diffraction-limited performance vertically. Reduced horizontal beta functions at ID locations enhance phase-space matching and brilliance. For hard X-rays, substantial improvements in brilliance and coherence are expected, particularly with IVUs and CPMUs. Optimal performance occurs at intermediate coupling levels, balancing intra-beam scattering effects and phase-space matching.

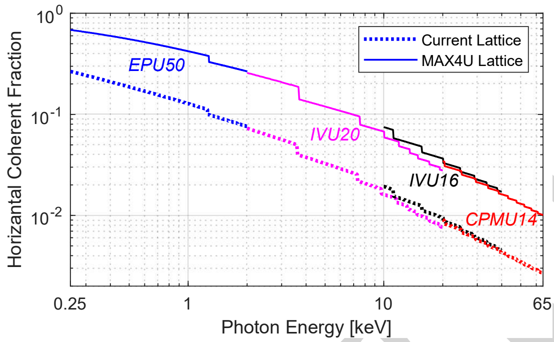

Figure 6: Horizontal coherent fraction comparison of R3 and MAX 4^U based on used ID technologies at MAX IV.

PLANNING AND INSTALLATION

Installation of MAX 4^U is planned to begin at the start of 2031 summer shutdown and will finish within 6 months. The ring tunnel is sectioned into five radiologically controlled areas, with one being shared with the 1.5 GeV ring and the SPF. Since these accelerators will be in normal operations, installation work in this section must be completed during the regular summer shutdown. This means that the installation work will start with the three achromats within that area. Full parallelism across these achromats is vital to stay within the time-constraint of the shutdown.

The installation work for the remaining 17 achromats will be carried out by two teams. One team will start at achromat #03 and the other at #12, both working clockwise around the ring. The tunnel installation work is expected to take six months to complete.

Once this phase is complete, it will be followed by three months of subsystem tests and a further three months of commissioning with beam, meaning that the dark period is estimated at 12 months. A planning envelope of 14 months has been allocated, providing a buffer of two months.

CONCLUSION

MAX 4^U is a major upgrade of the MAX IV 3 GeV storage ring, with the goal of reducing the natural bare-lattice emittance from its current value of 328 pm rad to an emittance below 75 pm rad. This paper outlines the ongoing accelerator physics and engineering studies, simulations, and prototyping efforts supporting its development.

ACKNOWLEDGMENTS

The authors would like to sincerely thank the MAX IV staff for their valuable input, creative ideas and contributions, and strong commitment to the design of MAX 4^U.

REFERENCES

[1] P. F. Tavares *et al.*, "The MAX IV storage ring project", *J. Synchrotron Radiat.*, vol. 21, pp. 862–877, Sep. 2014. doi:10.1107/S1600577514011503

[2] MAX 4U Conceptual Design Report (CDR), MAX IV Laboratory, Lund, Sweden, Dec. 2025, https://www.maxiv.lu.se/beamlines-accelerators/max-4u/accelerator-design/.

[3] E. Al-Dmour *et al.*, "MAX 4U: an upgrade of the MAX IV 3 GeV ring", in *Proc. IPAC'25*, Taipei, Taiwan, Jun. 2025, pp. 752–755. doi:10.18429/JACoW-IPAC2025-MOPS061

[4] M. Apollonio *et al.*, "Beam dynamics studies for the MAX 4U lattices", presented at IPAC'26, Deauville, France, May 2026, paper THP2115, this conference.

[5] A. Terebilo, "Accelerator modeling with MATLAB accelerator toolbox", in *Proc. PAC'01*, Chicago, IL, USA, Jun. 2001, paper RPAH314, pp. 3203–3205.

[6] J. Bengtsson, Tracy 3.5, https://github.com/jbengtsson/tracy-3.5/.

[7] J. Bengtsson, Thor-2.0, https://github.com/jbengtsson/thor-2.0/.

[8] P. Schnizer *et al.*, "Progress on Thor SCSI development", in *Proc. IPAC'23*, Venice, Italy, May 2023, pp. 3413–3416. doi:10.18429/JACoW-IPAC2023-WEPL127

[9] M. Borland, "elegant: A Flexible SDDS-compliant code for accelerator simulation", Advanced Photon Source LS-287, September 2000.

[10] A. Streun, "OPA Lattice design code", https://github.com/opa-code/opa-4/.

[11] M. B. Alves *et al.*, "Bunch lengthening with double- and triple-rf systems for MAX 4U", presented at IPAC'26, Deauville, France, May 2026, paper WEV5002, this conference.

[12] H. O. C. Duarte *et al.*, "Conceptual magnet designs for MAX 4U", presented at IPAC'26, Deauville, France, May 2026, paper MOP7068, this conference.

[13] A. Sharma *et al.*, "Design overview and project status of the PM gradient dipole at MAX IV", presented at IPAC'26, Deauville, France, May 2026, paper MOP7164, this conference.

[14] S. Thorin *et al.*, "The MAX IV Linac", in *Proc. LINAC'14*, Geneva, Switzerland, Aug.–Sep. 2014, pp. 400–403.

[15] D. Olsson *et al.*, "A chopper system for the MAX IV thermionic pre-injector", *Nucl. Instrum. Methods Phys. Res. A*, vol. 759, pp. 29–35, Sep. 2014. doi:10.1016/j.nima.2014.05.052

[16] P. Alexandre *et al.*, "Transparent top-up injection into a fourth-generation storage ring", *Nucl. Instrum. Methods Phys. Res. A*, vol. 986, p. 164739, Jan. 2021. doi:10.1016/j.nima.2020.164739

[17] M. Aiba *et al.*, "Longitudinal injection scheme using short pulse kicker for small aperture electron storage rings", *Phys. Rev. Spec. Top. Accel. Beams*, vol. 18, p. 020701, Feb. 2015. doi:10.1103/PhysRevSTAB.18.020701

[18] A. Dixon *et al.*, "Off-phase injection simulations for MAX 4U", presented at IPAC'26, Deauville, France, May 2026, paper THP2049, this conference.

[19] Å. Andersson *et al.*, "The 100 MHz RF System for the MAX IV Storage Rings", in *Proc. IPAC'11*, San Sebastian, Spain, Sep. 2011, pp. MOPC051, pp. 193–195.

[20] M. Grabski *et al.*, "Vacuum System of MAX 4U – An upgrade of MAX IV 3 GeV storage ring", in *Proc. IPAC'25*, Taipei, Taiwan, June 2025, pp. 2503-2506. doi:10.18429/JACoW-IPAC2025-THPB002

[21] M. Grabski *et al.*, "Commissioning and operation status of the MAX IV 3 GeV storage ring vacuum system", *J. Synchrotron Radiat.*, vol. 28, pp. 718-731, May 2021. doi:10.1107/s1600577521002599

[22] E. Al-Dmour *et al.*, "Diffraction-limited storage ring vacuum technology", *J. Synchrotron Radiat.*, vol. 21, pp 878-883, Sep. 2014. doi:10.1107/s1600577514010480

[23] K. Åhnberg *et al.*, "Mechanical evaluation and CAD modelling for MAX 4U: MAX IV storage ring upgrade", in *Proc. MEDSI'25*, Lund, Sweden, Sep. 2025, pp. 244–246. doi:10.18429/JACoW-MEDSI2025-WEP47

PREPRINT